

CNA-TTA: Clean and Noisy Region Aware Feature Learning within Clusters for Online-Offline Test-Time Adaptation

Hyeonwoo Cho^{1*}

Chanmin Park^{1*}
VUNO Inc¹

Jinyoung Kim¹
POSTECH²

Won Hwa Kim²

{hyeonwoo.cho, chanmin.park, jinyoung.kim}@vuno.co

wonhwa@postech.ac.kr

Abstract

A domain shift occurs when training (source) and test (target) data diverge in their distribution. Test-time adaptation (TTA) addresses the domain shift problem, aiming to adopt a trained model on the source domain to the target domain in a scenario where only a well-trained source model and unlabeled target data are available. In this scenario, handling false labels in the target domain is crucial because they negatively impact the model performance. To deal with this problem, we propose to utilize cluster structure (i.e., ‘Clean’ and ‘Noisy’ regions within each cluster) in the target domain formulated by the source model. Given an initial clustering of target samples, we first partition clusters into ‘Clean’ and ‘Noisy’ regions defined based on cluster prototype (i.e., centroid of each cluster). As these regions have totally different distributions of the true pseudo-labels, we adopt distinct training strategies for the clean and noisy regions: we selectively train the target with clean pseudo-labels in the clean region, whereas we introduce mixup inputs representing intermediate features between clean and noisy regions to increase the compactness of the cluster. We conducted extensive experiments on multiple datasets in online/offline TTA settings, whose results demonstrate that our method, CNA-TTA, achieves state-of-the-art for most cases.

1. Introduction

Domain shift occurs when training (source) and testing (target) data diverge in their distributions, and a trained model fails to generalize on the target data. Unsupervised Domain Adaptation (UDA) methods [6, 15, 37, 50, 61] deal with the shift, assuming that one has access to both the source and target data and aligns their distributions. However, such a scenario is not feasible in many real-world cases where privacy issues or regulations prevent access to the source data (e.g., healthcare data or autonomous vehicles). Consequently, Test-Time Adaptation (TTA) or Source-Free Unsupervised

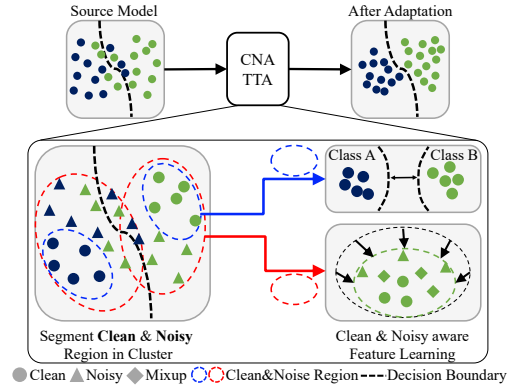


Figure 1. Illustration of CNA-TTA. The upper left presents the feature distribution of the target domain from a source model. The upper right shows the feature distribution of the target domain after applying CNA-TTA. The bottom depicts the process of CNA-TTA.

Domain Adaptation (SFUDA) [4, 27, 34, 58, 73] has been proposed and studied, which utilizes the knowledge from a pre-trained source model and unlabeled target data.

Recent advancements in TTA/SFUDA primarily employ self-training methods [4, 27, 34, 36, 64, 73]. These techniques allow a source model to learn the target domain’s knowledge using pseudo-labels generated in the target domain and predominantly focus on generating reliable pseudo-labels from the neighborhood structure within the feature space. However, due to the domain shift, there are several ambiguous and noisy samples. Directly utilization of their noisy pseudo-labels in training can adversely impact the model; hence, distinguishing and appropriately managing clean and noisy pseudo-labels is highly critical.

Our preliminary studies, as well as other literature [7, 70, 72] have shown that samples with noisy pseudo-labels are mostly observed at cluster boundaries, as shown in Fig. 1, underscoring the importance of considering clean and noisy pseudo-labels separately for each cluster. Several recent self-training methods [27, 53] employ selective pseudo-labeling for TTA to focus on reliable pseudo-labels for training. They neglect the target samples with unreliable pseudo-labels, aiming to transfer the knowledge from the target domain to

*Equal contribution

the source model only through reliable but limited pseudo-labels. To fully exploit the knowledge of the target domain, it is also vital to effectively learn from unreliable pseudo-labels as much as possible. Therefore, our key idea is to design a test-time adaptation method that effectively learns both clean and noisy pseudo-labels in an unseen target domain, thereby enabling the source model to represent the target domain’s knowledge better.

In this work, we introduce Clean and Noisy region Aware TTA, namely CNA-TTA, a novel TTA approach that focuses on addressing pseudo-labels of samples near cluster boundaries given the domain knowledge from a source model. We first partition Clean and Noisy regions within clusters formed in the target domain by leveraging cluster prototype (i.e., the centroid of each cluster) to measure the distance between the prototypes and the unlabeled target samples. Then, as illustrated in the bottom right of Fig. 1, distinct training strategies are adopted for the clean and noisy regions due to their divergent local characteristics.

For the clean region, we conduct selective training using reliable pseudo-labels derived from predictions of the nearest neighborhoods. In the noisy region, we leverage mixup inputs that represent intermediate features bridging clean and noisy regions in Fig. 1, unlike other methods that directly employ or discard the unreliable pseudo-labels for training. To draw these mixup inputs towards the clean region effectively, we introduce a mixed-clean probability, thereby enabling effective training on samples in noisy regions. Finally, in order to generate reliable pseudo-labels, we introduce the contrastive learning framework, aligning the nearest features effectively. Our method utilizes instance-discriminate and class-semantic features by introducing the memory bank [18] and the cluster prototype embedding through contrastive learning.

To summarise, the main contributions of our work are:

- We propose CNA-TTA, the novel TTA approach that focuses on handling pseudo-labels by utilizing cluster structure information in the target domain driven by a source model.
- We employ distinct training strategies for the clean and noisy regions due to their discriminate characteristics in the reliable pseudo-label distributions.
- We extensively validate CNA-TTA on various benchmarks for online/offline TTA in single-source and multi-source settings. In the end, CNA-TTA outperforms the SOTA techniques by a large margin in the challenging setting of online/offline TTA.

2. Related Work

2.1. Unsupervised Domain Adaptation

Unsupervised Domain Adaptation (UDA) [15, 37] has been widely proposed to address the domain shift problem. Adversarial learning methods, as in [5, 9, 15, 38, 55, 71], are a primary approach, focusing on aligning distribution discrepancies between the source and the target domains. Another approach proposed by [30, 50] introduces a discrepancy metric, which is used to minimize discrepancies in both the source and target distributions. Generative methods [2, 42, 44] have been utilized to tackle the domain shift by generating images that are indistinguishable between the source and target domains. In addition, [12, 54] have explored the utilization of cluster structure information to understand class relationships between instances with the help of the labeled source data. More recently, self-training methods [6, 7, 19, 40, 59, 68, 75] produce pseudo-labels for the target data to transfer the target domain’s knowledge to the source model. However, all these UDA approaches require access to both source and target data during the adaptation.

2.2. Source-Free and Test-Time Adaptation

Recently, several methods [4, 27, 34, 36, 58, 73] have been proposed for handling the test-time shift in source-free unsupervised domain adaptation (SFUDA) and online test-time adaptation (TTA) settings. Tent [58] optimizes entropy minimization for online TTA. SHOT [34], as a self-training method, introduces a class centroid used for pseudo-labeling for SFUDA. As another approach, CoWA-JMDS [31] utilizes the joint model-data structure as sample-wise weights to represent target domain knowledge effectively. CRCo [73] proposes a probability-based similarity between target samples by embedding the source domain class relationship.

In particular, some self-training approaches [4, 18, 66] are proposed for TTA/SFUDA. AdaContrast [4] proposes contrastive learning based on MoCo [18] and online pseudo-labeling, leveraging the consistency of predictions between local neighbors for TTA. Similarly, AaD [66] introduces contrastive learning using consistency between local neighbor features. C-SFDA [27] proposes a curriculum learning-aided self-training framework to obtain reliable samples for pseudo-labeling.

These self-training methods for TTA/SFUDA utilize local neighbor features to obtain reliable pseudo-labels in the target domain. However, a limitation of these methods is that they do not consider cluster structure information in the target domain, potentially leading to the learning of unreliable pseudo-labels for samples near cluster boundaries. In this work, we partition clean and noisy regions within a cluster (i.e., cluster structure information) and focus on addressing noisy pseudo-labels of samples around cluster boundaries.

3. The Proposed Method

In this work, we address Test-Time Adaptation (TTA) for the image classification task. In TTA, we are given a source model trained on labeled source data $\mathcal{D}_s = \{x_s^i, y_s^i\}_{i=1}^{N_s}$ and unlabeled target data $\mathcal{D}_t = \{x_t^i\}_{i=1}^{N_t}$, where x_s^i, x_t^i represent the input images and N_s, N_t denote the numbers of data in the source and target domains, respectively. We focus on the closed-set test-time adaptation where the target domain shares the same C classes as the source domain.

Given a pre-trained source model $f(\cdot)$ only, the objective of TTA is to adapt the model to work on the unlabeled target data \mathcal{D}_t . We assume a general architecture of the source model $f(\cdot) = h(g(\cdot))$ comprising an encoder $g(\cdot)$ and a classifier $h(\cdot)$, and our method is introduced below.

Overview In the test-time adaptation phase, we employ MoCo framework following [4]. We initialize the momentum model $\bar{f}(\cdot) = \bar{h}(\bar{g}(\cdot))$ with the parameters from the source model $f(\cdot)$ at the beginning of adaptation, and $\bar{f}(\cdot)$ is updated by the exponential moving average of the source encoder $g(\cdot)$ and the source classifier $h(\cdot)$ at each mini-batch step to enhance the stability of the feature space. As illustrated in Fig. 2, the source encoder $g(\cdot)$ and the momentum encoder $\bar{g}(\cdot)$ take input images $\{\mathcal{T}(x_t^i)\}_{i=1}^{N_t}$ from the target domain $\{x_t^i\}_{i=1}^{N_t}$ with weak and two strong augmentations $\mathcal{T} = \{T_w, T_s, T_{\bar{s}}\}$ and mixed images $\mathcal{D}_{mix} = \{\tilde{x}_t^i\}_{i=1}^{N_t}$ generated from $\{x_t^i\}_{i=1}^{N_t}$, respectively.

Then, for the purpose of categorizing the target data into individual clusters, we produce pseudo-labels $\{\hat{y}_t^i\}_{i=1}^{N_t}$ for the target data via a nearest neighbor soft voting [41] in a memory queue Q_w , representing the target feature space. As depicted in Fig 2 (a), to filter the target samples with noisy pseudo-labels \hat{y}_t^i in each cluster, we partition the clusters into clean (close to μ_k) and noisy (far from μ_k) regions using a clean probability derived via the distance from the cluster prototype μ_k (i.e., centroid for k -th cluster).

Next, to leverage different characteristics of the clean and noisy regions, we employ distinct training strategies for each region. For samples in the clean regions, we train $g(\cdot)$ and $h(\cdot)$ on them with the clean pseudo-labels \hat{y}_t^i generated through nearest neighbors features, as shown in Fig. 2 (b). In contrast, for those in the noisy regions, we employ a cluster compactness learning strategy that incorporates mixup [69] between samples and the clean probability of each sample, as shown in (c) of Fig. 2.

Finally, as shown in Fig. 2 (d), to generate reliable \hat{y}_t^i from the nearest features, we adopt contrastive learning both between the prototype and sample embeddings, as well as among the samples themselves.

3.1. Clean and Noisy Regions in Clusters

In conventional DA (Domain Adaptation) scenarios, a significant domain discrepancy between the source and target domains often results in inaccurate pseudo-labels generated

via the source model, negatively impacting the model's performance on the target domain. In particular, TTA is more challenging compared to traditional DA, as it offers no access to the source data, and thus efficiently leveraging the knowledge of the target domain is critical. In this work, we utilize the cluster structure (i.e., clean and noisy regions within clusters) and cluster prototype μ_k in the target as the knowledge of the target domain.

To address this, we propose an approach that guides the model to learn the cluster structure in the feature space with respect to the prototypes of each cluster in the target domain. Initially, to enable efficient nearest-neighbor search for generating the pseudo-labels \hat{y}_t^i from the cluster structures, we store the features $w_t = g(T_w(x_t))$ and their class-wise probability $p_t = \sigma(f(T_w(x_t)))$ in a memory queue $Q_w = \{w_t^j, p_t^j\}_{j=1}^M$ of the length of M , where σ denotes the softmax function. Then, in order to assign the target images x_t into each cluster, we generate its pseudo-labels \hat{y}_t^i by performing a soft voting [41] among the K closest neighbors of x_t in Q_w . The soft voting is done by averaging their probability outputs as:

$$\hat{p}_t^{(i,c)} = \frac{1}{K} \sum_{j=1}^K p_t^{(j,c)}, \quad (1)$$

and \hat{y}_t^i is categorized into cluster c by using $\argmax_c \hat{p}_t^{(i,c)}$.

To determine whether a given target sample x_t^i is clean or noisy within the cluster, as shown (a) in Fig. 2, we introduce a Gaussian Mixture Model (GMM) [49]. Given the observation x_t^i , a probability of the latent variable z_i that x_t^i belongs to k -th cluster is defined as:

$$\gamma_{ik} = p(z_i = k | x_t^i) = \frac{\pi_k \mathcal{N}(x_t^i | \mu_k, \sigma_k)}{\sum_k \pi_k \mathcal{N}(x_t^i | \mu_k, \sigma_k)} \quad (2)$$

where z_i represents the assignment of each cluster, μ_k and σ_k indicate the mean and variance of the Gaussian distribution $\mathcal{N}(x_t^i | \mu_k, \sigma_k)$ for the k -th cluster, and π_k is the prior probability of cluster k , i.e., $p(z_i = k)$. Here, assuming that z_i has uniform distribution, the Eq. (2) is expressed as:

$$\gamma_{ik} = p(z_i = k | x_t^i) = \frac{\mathcal{N}(x_t^i | \mu_k, \sigma_k)}{\sum_k \mathcal{N}(x_t^i | \mu_k, \sigma_k)}, \quad (3)$$

whose μ_k, σ_k , and z_i can be solved via EM algorithm [49].

In this work, we hypothesize that x_t^i has a clean label if \hat{y}_t^i from our model and z_i estimated via the GMM are identical. To connect \hat{y}_t^i and z_i in GMM, we adopt the μ_k, σ_k , and z_i computed using $f(\cdot)$. Specifically, we represent our predictions $p(\hat{y}_t^i = k | x_t^i, \theta)$ as the posterior probability, along with the output feature $g(x_t^i)$ as the given observation. Thus, following [49], μ_k, σ_k are represented as:

$$\mu_k = \left\| \frac{\sum_i p(\hat{y}_t^i = k | x_t^i, \theta) g(x_t^i)}{\sum_i p(\hat{y}_t^i = k | x_t^i, \theta)} \right\|_{\ell_2}, \quad (4)$$

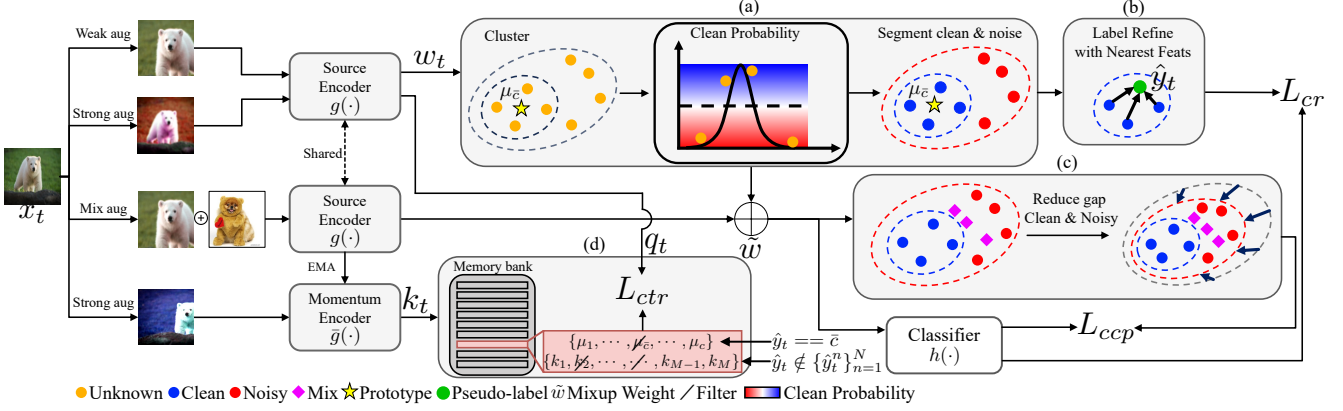


Figure 2. **Framework of CNA-TTA** Section (a): partition the cluster into ‘Clean’ (close to the cluster prototype) and ‘Noisy’ (far from the cluster prototype) region based on the clean probability distribution. Section (b): training samples in clean regions with pseudo-labels generated from prediction of closest features. Section (c): reducing a gap between clean and noisy region with mixup weight. Section (d): prototype-aware and instance-aware contrastive learning.

$$\sigma_k = \frac{\sum_i p(\hat{y}_t^i = k | x_t^i, \theta) (g(x_t^i) - \mu_k)^T (g(x_t^i) - \mu_k)}{\sum_i p(\hat{y}_t^i = k | x_t^i, \theta)}. \quad (5)$$

With the above parameters μ_k, σ_k estimated from $f(\cdot)$, the Eq. (3) is defined by the probability density function:

$$\begin{aligned} \gamma_{ik} &= \frac{\exp(-(g(x_t^i) - \mu_k)^T (g(x_t^i) - \mu_k) / 2\sigma_k)}{\sum_k \exp(-(g(x_t^i) - \mu_k)^T (g(x_t^i) - \mu_k) / 2\sigma_k)} \\ &= \frac{\exp(g(x_t^i)^T \mu_k / \sigma_k)}{\sum_k \exp(g(x_t^i)^T \mu_k / \sigma_k)}. \end{aligned} \quad (6)$$

Thus, the probability of the sample being clean is defined as:

$$\gamma_{\hat{y}_t^i = z_i} = p(\hat{y}_t^i = z_i | x_t^i) = \frac{\exp(g(x_t^i)^T \mu_{z_i} / \sigma_{z_i})}{\sum_k \exp(g(x_t^i)^T \mu_k / \sigma_k)} \quad (7)$$

by using $g(x_t^i)^T \mu_k$ as the distance metric between the prototype and the sample embedding. From this probability distribution, our method enables the partition of each cluster into closer (Clean) and farther (Noisy) regions relative to the prototype through the probability threshold α . Thus, the samples in the clean and noisy region are represented as:

$$\{x_t^i\}_{i=1}^{N_t} = \begin{cases} \{x_t^{cr}\}_{cr=1}^{N_{cr}}, & \text{if } p(\hat{y}_t^i = z_i | x_t^i) \geq \alpha \\ \{x_t^{nr}\}_{nr=1}^{N_{nr}}, & \text{otherwise,} \end{cases} \quad (8)$$

where N_{cr} and N_{nr} denote the number of samples in clean and noisy regions.

3.2. Train Clean and Noisy region

In our preliminary study, we observed that the clean and noisy regions within a cluster have divergent local characteristics. In the clean region, the samples, as well as their closest features, have reliable pseudo-labels \hat{y}_t generated by Eq. 1, as they are also in the clean regions. On the other hand, the noisy regions contain samples with incorrect \hat{y}_t , as they are located near or on the cluster boundaries. To deal with this issue, we employ distinct training strategies for $\{x_t^{cr}\}_{cr=1}^{N_{cr}}$

and $\{x_t^{nr}\}_{nr=1}^{N_{nr}}$. In the clean region, we exclusively train on $\{x_t^{cr}\}_{cr=1}^{N_{cr}}$ with the pseudo-labels \hat{y}_t , as they are more reliable than \hat{y}_t for $\{x_t^{nr}\}_{nr=1}^{N_{nr}}$ from the noisy regions. The loss for the samples in the clean region is given by:

$$L_{cr} = -\mathbb{E}_{x_t^{cr} \in \mathcal{X}_t} \sum_{c=1}^C \hat{y}_t^c \log p_t^c. \quad (9)$$

For the noisy region, we avoid directly using \hat{y}_t for $\{x_t^{nr}\}_{nr=1}^{N_{nr}}$ for training but rather leverage mixup input \tilde{x}_t for the effective noisy training, as the mixup samples lie in between the stable and noisy samples. Inspired by [43], we consider $g(\tilde{x}_t)$ as the features to bridge the gap between the clean and noisy regions. Here, \tilde{x}_t^i and its pseudo-label \tilde{y}_t^i are represented as $\lambda x_t^i + (1 - \lambda)x_t^j$ and $\lambda \hat{y}_t^i + (1 - \lambda)\hat{y}_t^j$, where $\{x_t^i, x_t^j\} \in D_t$ and mixup ratio $\lambda \in [0, 1]$. To effectively attract \tilde{x}_t to the clean region, we introduce the mixed-clean probability $p(\tilde{y}_t^i = z_i | \tilde{x}_t^i)$, assigning greater significance as \tilde{x}_t^i approaches the clean region. We define $p(\tilde{y}_t^i = z_i | \tilde{x}_t^i)$ as a weighted sum of the clean probabilities of x_t^i and x_t^j :

$$p(\tilde{y}_t^i = z_i | \tilde{x}_t^i) = \lambda p(z_i | x_t^i) + (1 - \lambda)p(z_j | x_t^j). \quad (10)$$

We then represent the mixup weight, denoted as \tilde{w} , using $p(\tilde{y}_t^i = z_i | \tilde{x}_t^i)$ with an exponential function:

$$\tilde{w} = \exp(p(\tilde{y}_t^i = z_i | \tilde{x}_t^i)) \quad (11)$$

which varies depending on the regions where x_t^i and x_t^j are located by Eq. 10. If both x_t^i and x_t^j are in the noisy region, \tilde{w} has a low value and vice versa for the clean region. We argue that using \tilde{x}_t with \tilde{w} enhances the compactness of the cluster since the model can learn intermediate features between the clean and noisy region, as illustrated in (c) in Fig. 2. Together with the mixup samples, the Cluster ComPactness

(CCP) loss, denoted as L_{ccp} , is given by:

$$L_{ccp} = -\tilde{w} \cdot \mathbb{E}_{\tilde{x}_t \in \tilde{\mathcal{X}}_t} \sum_{c=1}^C \tilde{y}_t^c \log \tilde{p}_t^c, \quad (12)$$

where $\tilde{p}_t = \sigma(f(\tilde{x}_t))$ are the predicted probabilities for \tilde{x}_t .

Additionally, we add a regularization that promotes diverse predictions similar to [4] as:

$$L_{div} = \mathbb{E}_{x_t \in \mathcal{X}_t} \sum_{c=1}^C \bar{p}_t^c \log \bar{p}_t^c \quad (13)$$

where $\bar{p}_t = \mathbb{E}_{x_t \in \mathcal{X}_t} \sigma(f(T_s(x_t)))$ and the L_{div} prevents the model from trusting false pseudo-labels.

3.3. Instance and Prototype-aware Contrast

In our method, we generate the pseudo-labels of the target samples from the nearest features, as discussed in Eq. 1. However, the pseudo-labels might be incorrect if the predictions of their nearest features are not correlated with the class of the target. To better align the nearest features, we introduce the contrast learning framework. Prior approaches [22, 28, 46, 74] consider each pair of instances as attractive and dispersing samples to enable instance discrimination. However, the limitation of these approaches is that it is difficult to attract different instances with similar semantic features in the same cluster, thereby posing challenges in encoding class-semantic information between instances.

To address these challenges, we contrast the prototype μ_k obtained in Section 3.1 and queries $q_t = g(T_s(x_t))$ for prototype-aware contrastive learning. As described in Fig. 2 (d), we pair q_t and $\mu_{k=\bar{c}}$ (i.e., the prototype feature of corresponding class $\bar{c} = \hat{y}_t$ of q_t), as the positive pair. In contrast, the negative pair is given by q_t and $\{\mu_{k \neq \bar{c}}\}_{k=1}^C$, which are the prototype features not corresponding to class \bar{c} . Our prototype-aware contrastive loss is defined as:

$$L_{prt} = -\log \frac{\exp q_t \cdot \mu_{k=\bar{c}}/\tau}{\sum_{k \neq \bar{c}} \exp q_t \cdot \mu_k/\tau}, \quad (14)$$

and τ is a temperature controlling the scale of predictions.

Moreover, to learn instance-discriminate features, we leverage queries q_t and keys $k_t = \bar{g}(T_{\bar{s}}(x_t))$ as the positive pair as in [18]. To build the negative pairs \mathcal{N}_p of q_t , we store k_t to the memory queue $Q_k = \{k_t^i\}_{i=1}^M$ with the length M , but Q_k may have features which have the same class as the corresponding class \hat{y}_t of q_t . In our work, to eliminate negative pairs with the same class, we utilize the nearest feature information in Q_k . We exclude the negative pairs when classes $\{\hat{y}_t^n\}_{n=1}^N$ of their N closest features are at least one the same as \hat{y}_t , as shown in Fig. 2 (d). Our instance-aware contrastive loss reflecting the behavior above is given by:

$$L_{inst} = -\log \frac{\exp q_t \cdot k_t/\tau}{\sum_{j \in \mathcal{N}_p} \exp q_t \cdot k_j^j/\tau} \quad (15)$$

where \mathcal{N}_p is defined as $\{j | 1 \leq j \leq M, \hat{y}_t^j \notin \{\hat{y}_t^n\}_{n=1}^N\}$, and the overall contrastive loss combining L_{prt} and L_{inst} is expressed as:

$$L_{ctr} = L_{inst} + L_{prt}. \quad (16)$$

In the end, by summarizing all the losses from (9), (12), (13) and (16), we get the global loss function as below:

$$L_{overall} = \gamma_1 L_{cr} + \gamma_2 L_{ccp} + \gamma_3 L_{div} + \gamma_4 L_{ctr}, \quad (17)$$

and we set $\gamma_1 = \gamma_2 = \gamma_3 = \gamma_4 = 1.0$ during training.

4. Experiments

4.1. Experimental Setup

Datasets. VisDA-C [47] is a large-scale dataset consisting of 12 classes for Synthetic-to-Real object classification. The source domain has 152k synthetic images, while the target domain has 55k real-world images. We compare the per-class top-1 accuracies and their class-wise averages. **DomainNet-126** is a subset of DomainNet [48], comprising 4 domains: Real (R), Sketch (S), Clipart (C), and Painting (P) with 126 classes, following the setup in [51]. **PACS** [32] has 4 domains: Art-Painting (A), Cartoon (C), Photo (P), and Sketch (S) with 7 classes. For DomainNet-126 and PACS, we compare the accuracy for each domain shift and the average of all domain shifts. We will perform experiments that deal with the domain shifts within each dataset.

Architecture For a fair comparison with prior methods, we adopt the same architectures and training strategies for the source model. Specifically, we use ResNet [17] as our backbones: ResNet-18 for PACS, ResNet-50 for DomainNet-126, and ResNet-101 for the VisDA-C. We add a 256-dimensional bottleneck layer, which is a fully-connected layer, followed by BatchNorm [23] after the backbone, and apply Weight-Norm [52] to the classifier, as done in [4, 34, 36].

Implementation details. For the source training, we initialize the model with ImageNet-1K [11] pre-trained weights. We train the pre-trained model on the source data, the same as in [4]. For offline TTA, we opt for the SGD optimizer with a momentum of 0.9 and a learning rate of $2e-4$ for all datasets. We set the threshold α of the clean probability to 0.5, the temperature τ to 0.07, the memory bank size M to 16384, and the momentum value for the EMA update to 0.999. For online TTA, we turn on/off a soft-voting for pseudo labeling when 1024 features-probability pairs are accumulated in the memory queue. Other hyper-parameters are the same as in offline TTA. More details in Appendix.

4.2. Experimental Results

Tab. 1, 2, and 3 show the performance of CNA-TTA and the compared methods across 3 different datasets in the single-source setting. Tab. 4 shows results in the multi-source setting. In each table, † indicates the results that we reproduced

Method	SF	plane	bicycl	bus	car	horse	knife	mcycl	person	plant	sktbrd	train	truck	Avg.
MCC(ECCV'20)[25]	✗	88.7	80.3	80.5	71.5	90.1	93.2	85.0	71.6	89.4	73.8	85.0	36.9	78.8
RWOT(CVPR'20) [63]	✗	95.1	80.3	83.7	90.0	92.4	68.0	92.5	82.2	87.9	78.4	90.4	68.2	84.0
SE (ICLR'18) [14]	✗	95.9	87.4	85.2	58.6	96.2	95.7	90.6	80.0	94.8	90.8	88.4	47.9	84.3
CAN (CVPR '19) [26]	✗	97.0	87.2	82.5	74.3	97.8	96.2	90.8	80.7	96.6	96.3	87.5	59.9	87.2
Source Only	-	57.2	11.1	42.4	66.9	55.0	4.4	81.1	27.3	57.9	29.4	86.7	5.8	43.8
SHOT (ICML'20) [34]	✓	95.3	87.5	78.7	55.6	94.1	94.2	81.4	80.0	91.8	90.7	86.5	59.8	83.0
G-SFDA (ICCV'21) [65]	✓	96.1	88.3	85.5	74.1	97.1	95.4	89.5	79.4	95.4	92.9	89.1	42.6	85.4
NRC (NeurIPS'21) [64]	✓	96.8	91.3	82.4	62.4	96.2	95.9	86.1	80.6	94.8	94.1	90.4	59.7	85.9
SFDA-DE (CVPR'22) [13]	✓	95.3	91.2	77.5	72.1	95.7	97.8	85.5	86.1	95.5	93.0	86.3	61.6	86.5
CoWA-JMDS (ICML'22) [31]	✓	96.2	89.7	83.9	73.8	96.4	<u>97.4</u>	89.3	<u>86.8</u>	94.6	92.1	88.7	53.8	86.9
AdaContrast [†] (CVPR'22) [4]	✓	97.2	83.6	84.0	77.2	96.9	94.4	91.6	84.9	94.5	93.3	<u>94.1</u>	45.9	86.5
NRC++ (TPAMI'23) [64]	✓	97.4	91.9	<u>88.2</u>	<u>83.2</u>	97.3	96.2	90.2	81.1	96.3	<u>94.3</u>	91.4	49.6	88.1
C-SFDA [†] (CVPR'23) [27]	✓	<u>97.6</u>	88.8	86.1	72.2	97.2	94.4	92.1	84.7	93.0	90.7	93.1	63.5	87.8
AaD-SFDA [†] (NeurIPS'22) [66]	✓	97.4	90.5	80.8	76.2	<u>97.3</u>	96.1	89.8	82.9	95.5	93.0	92.0	<u>64.7</u>	88.0
GU-SFDA [†] (CVPR'23) [36]	✓	97.1	<u>91.2</u>	87.6	72.1	96.9	96.4	<u>93.8</u>	86.7	<u>96.3</u>	94.2	91.3	67.0	<u>89.2</u>
CNA-TTA (Ours)	✓	98.0	90.2	91.3	88.9	98.1	96.2	94.7	88.6	97.7	97.3	95.3	49.5	90.5
AdaContrast [†] (online) (CVPR'22) [4]	✓	95.0	68.0	82.7	<u>69.6</u>	94.3	80.8	90.3	79.6	<u>90.6</u>	69.7	<u>87.6</u>	36.0	78.7
C-SFDA [†] (online) (CVPR'23) [27]	✓	<u>95.9</u>	<u>75.6</u>	<u>88.4</u>	68.1	<u>95.4</u>	<u>86.1</u>	94.5	<u>82.0</u>	89.2	<u>80.2</u>	87.3	43.8	<u>82.1</u>
CNA-TTA (Ours) (online)	✓	96.7	82.2	89.3	82.7	96.9	94.8	<u>94.2</u>	86.6	94.9	91.4	89.8	<u>42.3</u>	86.8

Table 1. Classification Accuracy (%) on **VisDA-C** for Single-Source Domain Adaptation (ResNet-101 backbone). The highest is bold, the second is underlined, and our method is highlighted.

Method	SF	R → C	R → P	P → C	C → S	S → P	R → S	P → R	Avg
MCC [25]	✗	44.8	65.7	41.9	34.9	47.3	35.3	72.4	48.9
Source Only	-	55.5	62.7	53.0	46.9	50.1	46.3	75.0	55.6
SHOT [34]	✓	67.7	68.4	66.9	60.1	66.1	59.9	<u>80.8</u>	67.1
AdaContrast [†] [4]	✓	69.7	69.0	68.6	58.4	66.6	60.5	80.2	67.6
C-SFDA [†] [27]	✓	70.8	<u>71.1</u>	68.5	<u>62.1</u>	67.4	<u>62.7</u>	80.4	69.0
GU-SFDA [†] [36]	✓	74.2	70.4	68.8	64.0	<u>67.5</u>	65.7	76.5	69.6
CNA-TTA (Ours)	✓	<u>73.7</u>	72.2	71.7	60.6	67.8	64.7	83.2	70.4
TENT(online) [58]	✓	58.5	65.7	57.9	48.5	52.4	54.0	67.0	57.7
AdaContrast [†] (online) [4]	✓	61.1	66.9	60.8	53.4	62.7	64.5	78.9	62.6
C-SFDA [†] (online) [27]	✓	61.6	67.4	61.3	<u>55.1</u>	63.2	54.8	<u>78.5</u>	<u>63.1</u>
CNA-TTA(online)	✓	67.1	69.0	65.6	59.1	66.4	<u>59.9</u>	81.5	66.9

Table 2. Classification Accuracy (%) on **DomainNet-126** for Single-Source Domain Adaptation (ResNet-50 Backbone).

Method	SF	P → A	P → C	P → S	A → P	A → C	A → S	Avg
Source Only	-	58.0	21.1	27.8	96.1	48.6	39.7	48.6
NEL [1]	✓	82.6	<u>80.5</u>	32.3	<u>98.4</u>	<u>84.3</u>	56.1	72.4
GU-SFDA [†] [36]	✓	<u>88.6</u>	82.2	69.0	96.3	84.6	<u>73.9</u>	82.4
CNA-TTA (Ours)	✓	92.2	69.1	<u>66.2</u>	98.8	83.0	84.8	82.4
CNA-TTA (online)	✓	76.3	64.4	60.7	97.1	74.9	73.3	74.4

Table 3. Classification Accuracy (%) on **PACS** for Single-Source Domain Adaptation (ResNet-18 Backbone).

from the released source code, and ‘SF’ denotes ‘source-free’. All reported results are average accuracies from three seeds.

Single-Source Domain Adaptation Tab. 1, 2, and 3 show the classification accuracy of CNA-TTA and previous methods for UDA and SFUDA in an offline setting. In Tab. 1, CNA-TTA outperforms UDA methods such as CAN [26], even without access to the source data. In the more challenging SFUDA, we surpass SOTA [36] by a 1.3% margin on per-class average accuracy in VisDA-C (Tab. 1) and by 0.8% margin on the average accuracy in DomainNet-126 (Tab. 2). In addition, in PACS (Tab. 3), we achieve competi-

tive performance compared to the SOTA. The self-training methods, such as AdaContrast [4] and GU-SFDA [36], utilize the nearest features to generate reliable pseudo-labels without considering cluster structure for SFUDA. We believe that CNA-TTA is more effective than these methods since our method addresses the pseudo-labels based on the clean probabilities within the cluster.

Method	SF	→ A	→ C	→ P	→ S	Avg
SIB (ICLR'20) [20]	✗	88.9	89.0	98.3	82.2	89.6
T-SVDNET (ICCV'21) [33]	✗	90.4	90.6	98.5	85.4	91.2
iMSDA (ICML'22) [29]	✗	93.7	92.4	98.4	89.2	93.4
Source Only	-	77.9	72.8	95.7	63.5	77.5
SHOT [†] (ICML'20) [34]	✓	90.7	88.1	98.5	75.4	88.2
SHOT++ [†] (TPAMI'21) [35]	✓	<u>92.3</u>	<u>89.7</u>	98.8	<u>75.5</u>	<u>89.1</u>
CNA-TTA (Ours)	✓	93.7	93.3	<u>98.7</u>	87.8	93.4
SHOT-IM [†] (online) (ICML'20) [60]	✓	<u>85.6</u>	<u>83.4</u>	96.8	68.4	83.6
TENT [†] (online) (ICLR'21) [58]	✓	81.3	81.2	96.1	74.8	83.4
T3A [†] (online) (NeurIPS'21) [24]	✓	79.0	79.8	96.2	68.7	81.0
TSDF [†] (online) (CVPR'23) [60]	✓	87.6	88.1	97.0	<u>78.5</u>	87.8
CNA-TTA (Ours) (online)	✓	82.6	82.5	<u>96.9</u>	84.0	<u>86.5</u>

Table 4. Classification Accuracy (%) on PACS for Multi-Source Unsupervised Domain Adaptation (ResNet-18 Backbone).

Multi-Source Domain Adaptation Table 4 presents the performance of Multi-Source Unsupervised Domain Adaptation (MSUDA) on PACS in an offline setting. In MSUDA, we treat each domain as the target domain and train the source model by aggregating all other domains without using domain labels. In a challenge source-free MSUDA, CNA-TTA achieves the highest accuracy on PACS. SHOT++ [35] produces pseudo-labels of the target based on the centroid of the nearest cluster. In contrast, CNA-TTA trains pseudo-labels for the target data with different strategies depending on whether the data is in clean or noisy regions. These results

demonstrate that CNA-TTA outperforms prior source-free MSUDA methods in terms of learning pseudo-label.

Online Test-Time Adaptation In Tab. 1, 2, 3, and 4, ‘on-line’ results show the classification accuracy of the proposed CNA-TTA and the compared methods for online TTA. In this protocol, the target domain’s data is seen to the model only once during the inference phase. In Tab. 1, 2, CNA-TTA significantly outperforms the SOTA methods (4.7% and 3.8% improvements in VisDA-C and DomainNet-126). C-SFDA [27] may fail to capture all the knowledge from the target domain, particularly from the noisy data, due to its selective approach based on curriculum learning. However, CNA-TTA can utilize the entire target domain’s knowledge by training effectively all samples. Additionally, Tab. 3 and Tab. 4 demonstrate the effectiveness of CNA-TTA in both single-source and multi-source settings on PACS. These results establish CNA-TTA as a more effective TTA method for challenging online TTA scenarios.

4.3. Analysis and Discussion

Ablation study on each component in CNA-TTA. Tab. 5 shows the effectiveness of each component on all datasets. The ‘PL’ method as a baseline indicates the method generating the pseudo-labels from nearest neighbors features in Eq. 1. As shown in Tab. 5, we apply each module in CNA-TTA one by one. By applying ‘ L_{cr} ’ in Sec. 3.2, we boost the performance by 3.1%, 7.3%, and 3.1% on VisDA-C, DomainNet-126, and PACS. These results confirm that ‘ L_{cr} ’ learning only the samples with clean labels is more effective than ‘PL’ using all data for training. Plus, the inclusion of the cluster compactness loss ‘ L_{ccp} ’ in Sec. 3.2 improves the performance on the target domains across all datasets. Finally, our contrastive losses ‘ L_{inst} ’, ‘ L_{prt} ’ in Sec. 3.3 consistently contribute to performance improvement on all datasets.

PL	L_{cr}	L_{ccp}	L_{div}	L_{inst}	L_{prt}	VisDA-C	DomainNet	PACS
✓	✗	✗	✗	✗	✗	84.9	58.5	75.7
✓	✓	✗	✗	✗	✗	88.0	65.8	78.8
✓	✓	✓	✗	✗	✗	89.6	67.4	79.7
✓	✓	✓	✓	✗	✗	89.0	67.7	80.6
✓	✓	✓	✓	✓	✗	90.1	69.7	81.1
✓	✓	✓	✓	✓	✓	90.5	70.4	82.4

Table 5. The effectiveness of each component across **all datasets** is validated by classification accuracy (%).

Effect on clean and noisy region in cluster. We demonstrate the effectiveness of partitioning clean and noisy data within clusters. In (a), (b) of Fig. 3, we present the feature distributions of the clean and noisy samples before and after applying CNA-TTA with t-SNE [56] on DomainNet-126. In the feature distributions, each pink and black triangular indicates noisy samples with correct noisy labels (i.e., Prediction: Noisy, Ground Truth: Noisy) and incorrect ones (i.e., Prediction: Noisy, Ground Truth: Clean). The green boxes in (a), (b) of Fig. 3 show that CNA-TTA correctly identifies clean

and noisy samples as the number of samples with incorrect noisy labels decreases. Notably, we present the examples of the samples with correct noisy labels in (c) of Fig. 3, and observe that they are hard samples to classify. Additionally, we evaluate the performance for detecting clean and noisy samples on all datasets, as shown in Fig. 4. The accuracy, recall, and precision for identifying samples as clean or noisy are presented with iterations. These performance metrics show improvement with iteration, even as the proportion of noisy samples decreases.

Linear vs Exponential weight. Tab. 6 demonstrates the effectiveness of the exponential weighting in Eq. 11, comparing linear one and without one. In particular, CNA-TTA shows performance improvement relative to previous TTA methods, even when linear weighting is utilized.

Method	VisDa-C	DomainNet	PACS
Ours w/o weighting	89.7	69.2	80.7
Ours w/ linear weighting	90.0	70.2	82.1
Ours w/ exponential weighting	90.5	70.4	82.4

Table 6. Classification Accuracy (%) on **all dataset** comparing linear vs exponential weighting in Eq. 11.

Similarity distribution of Clean vs Mixup vs Noisy. Fig. 5 presents the density distribution of similarity between clean, noisy, and mixup samples based on cluster prototypes on VisDA-C. We calculated this similarity using the cosine similarity between each sample’s embedding and its closest cluster prototype embedding. We observe that clean samples exhibit features closer to the prototype, while noisy samples exhibit more distant features. Notably, features of mixup tend to be distributed between the clean and noisy distributions. These findings support our hypothesis that mixup features serve as a bridge connecting clean and noisy features.

Model calibration. We consider that model calibration in TTA enhances the reliability, robustness, and interpretability of the adapted target model, making it a crucial aspect of deploying machine learning solutions in dynamic environments. In Fig. 6, we compare the model calibration [10, 16, 45] for AdaContrast and CNA-TTA on VisDA-C. We divide the

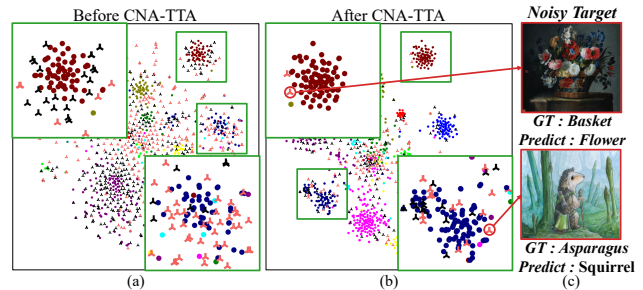


Figure 3. (a), (b) Visualization for clean (circle) and noisy (triangular) samples in feature space. For clean samples, colors represent classes. For noisy ones, pink and black triangular represent correct and incorrect noisy label. (c) Examples with correct noisy label.

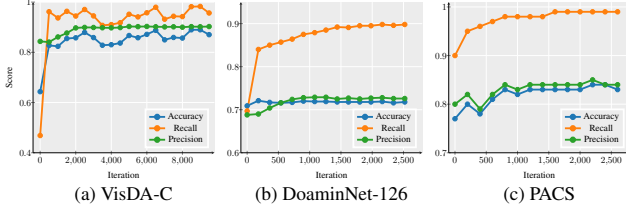


Figure 4. The performance for detecting clean and noisy data on all datasets.

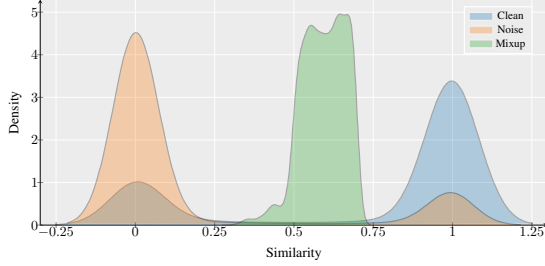


Figure 5. Similarity distribution of cluster prototype with Clean vs Noise vs Mixup.

probability of the model into 10 bins and compute the average accuracy in relation to the average confidence for each bin. The more close the model’s outputs (blue bar) to $y = x$ line, the better calibration it has. As shown in Fig. 6, CNA-TTA has better calibration than AdaContrast. In addition, we use two intuitive statistics that measure calibration [10, 45]: expected calibration error (ECE) and maximum calibration error (MCE). The more close ECE and MCE to zero, the better calibration the model has. CNA-TTA achieves 4.09(%) ECE and 1.47(%) MCE lower than AdaContrast’s.

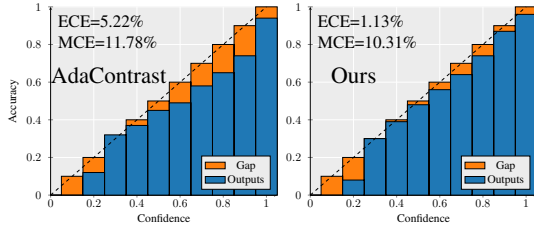


Figure 6. Model calibration analysis of AdaContrast [4] and CNA-TTA on VisDA-C.

Scalability on different models. In Tab. 7, we validate our method using different backbones to ensure it is the model-agnostic method. CNA-TTA outperforms better than the previous methods on PACS for MSUDA. Through these results, we confirm that our method works well with different backbones.

Compare with Domain Generalization. The goal of this analysis is to ensure generalization performance for an unseen target domain. To validate the effectiveness of CNA-TTA, we compare previous Domain Generalization methods.

BackBone	ResNet18	ResNet50	ViT-B/16
ERM [57]	82.1	84.6	87.1
RSC (ECCV’20)[21]	85.2	87.8	-
DGCM (ICML’21)[39]	85.5	87.5	-
FACT (CVPR’21)[62]	84.5	88.2	-
T3A (NeurIPS’21) [62]	81.7	84.5	86.0
TSD [†] (CVPR’23)[60]	87.8	89.4	90.2
CNA-TTA (Ours)	86.5	90.4	91.7

Table 7. Classification Accuracy on PACS with different backbone architecture for Multi-Source Unsupervised Domain Adaptation.

In Tab. 8, the results indicate that our method works well on the unseen target domain compared to other DG methods.

Method	→ A	→ C	→ P	→ S	Avg
ERM [57]	82.5	80.8	94.1	81.0	84.6
SWAD (NeurIPS’21) [3]	89.3	83.2	96.9	83.4	88.2
DNA (ICML’22) [8]	89.8	83.4	97.7	82.6	88.4
PCL (CVPR’22) [67]	90.2	83.9	98.1	82.6	88.7
CNA-TTA (Ours) (online)	89.6	87.3	98.9	85.9	90.4

Table 8. Classification Accuracy (%) on PACS for Domain Generalization (ResNet-50 Backbone).

Sensitivity of hyper-parameters. Fig. ?? shows that the hyper-parameters are insensitive to CNA-TTA. In particular, we investigate the robustness of CNA-TTA versus the clean probability threshold α and K in Eq. 14. In addition, we analyze the sensitivity of the memory queue length, which is the criterion for turning on and off soft voting for pseudo-labeling in the online TTA setting. These results demonstrate the insensitivity of CNA-TTA to the hyper-parameters.

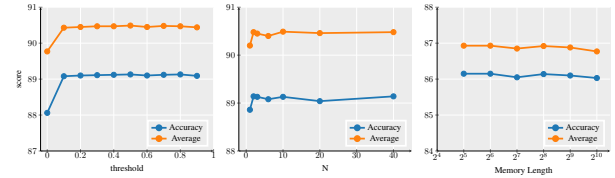


Figure 7. Sensitivity analysis of different hyper-parameters. Classification Accuracy (%) with the clean probability threshold α , N in Eq. 14, and a length of the memory queue turning a soft voting on and off for pseudo-labeling in online TTA setting.

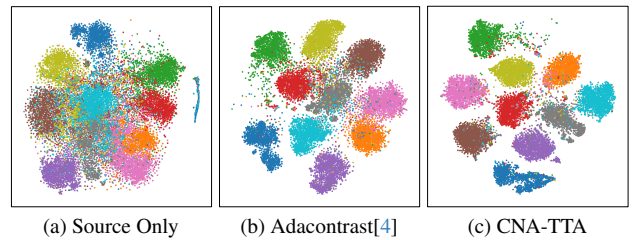


Figure 8. t-SNE of the feature distributions from ‘Source Only’, Adacontrast [4], and CNA-TTA on VisDA-C.

Feature Visualization. Fig. 8 shows the feature distributions from the source model (referred to as ‘Source Only’), Ada-Contrast [4] method, and CNA-TTA through t-SNE [56]. We

observe that the feature distribution of CNA-TTA has better cluster compactness than that of other methods.

5. Conclusion

We introduced CNA-TTA, a novel online-offline test time adaptation approach in image classification. To ensure the comprehensive transfer of target domain knowledge to the source model, effective learning of clean and noisy pseudo-labels from the target domain is crucial. To address this, we proposed distinguishing clean and noisy regions at the cluster level. Then, we apply different training strategies to each region by considering their respective characteristics. CNA-TTA surpassed the SOTA on major DA benchmarks by a significant margin, and further analyses demonstrated the efficacy of each proposed component.

References

- [1] Waqar Ahmed, Pietro Morerio, and Vittorio Murino. Cleaning noisy labels by negative ensemble learning for source-free unsupervised domain adaptation. In *Proceedings of the IEEE/CVF Winter Conference on Applications of Computer Vision*, pages 1616–1625, 2022. 6
- [2] Konstantinos Bousmalis, Nathan Silberman, David Dohan, Dumitru Erhan, and Dilip Krishnan. Unsupervised pixel-level domain adaptation with generative adversarial networks. In *Proceedings of the IEEE conference on computer vision and pattern recognition*, pages 3722–3731, 2017. 2
- [3] Junbum Cha, Sanghyuk Chun, Kyungjae Lee, Han-Cheol Cho, Seunghyun Park, Yunsung Lee, and Sungrae Park. Swad: Domain generalization by seeking flat minima. *Advances in Neural Information Processing Systems*, 34:22405–22418, 2021. 8
- [4] Dian Chen, Dequan Wang, Trevor Darrell, and Sayna Ebrahimi. Contrastive test-time adaptation. In *Proceedings of the IEEE/CVF Conference on Computer Vision and Pattern Recognition*, pages 295–305, 2022. 1, 2, 3, 5, 6, 8
- [5] Lin Chen, Huaian Chen, Zhixiang Wei, Xin Jin, Xiao Tan, Yi Jin, and Enhong Chen. Reusing the task-specific classifier as a discriminator: Discriminator-free adversarial domain adaptation. In *Proceedings of the IEEE/CVF Conference on Computer Vision and Pattern Recognition*, pages 7181–7190, 2022. 2
- [6] Hyeonwoo Cho, Kazuya Nishimura, Kazuhide Watanabe, and Ryoma Bise. Effective pseudo-labeling based on heatmap for unsupervised domain adaptation in cell detection. *Medical Image Analysis*, 79:102436, 2022. 1, 2
- [7] Jaehoon Choi, Minki Jeong, Taekyung Kim, and Changick Kim. Pseudo-labeling curriculum for unsupervised domain adaptation. *arXiv preprint arXiv:1908.00262*, 2019. 1, 2
- [8] Xu Chu, Yujie Jin, Wenwu Zhu, Yasha Wang, Xin Wang, Shanghang Zhang, and Hong Mei. Dna: Domain generalization with diversified neural averaging. In *International Conference on Machine Learning*, pages 4010–4034. PMLR, 2022. 8
- [9] Shuhao Cui, Shuhui Wang, Junbao Zhuo, Chi Su, Qingming Huang, and Qi Tian. Gradually vanishing bridge for adversarial domain adaptation. In *Proceedings of the IEEE/CVF conference on computer vision and pattern recognition*, pages 12455–12464, 2020. 2
- [10] Morris H DeGroot and Stephen E Fienberg. The comparison and evaluation of forecasters. *Journal of the Royal Statistical Society: Series D (The Statistician)*, 32(1-2):12–22, 1983. 7, 8
- [11] Jia Deng, Wei Dong, Richard Socher, Li-Jia Li, Kai Li, and Li Fei-Fei. Imagenet: A large-scale hierarchical image database. In *2009 IEEE conference on computer vision and pattern recognition*, pages 248–255. Ieee, 2009. 5
- [12] Zhijie Deng, Yucen Luo, and Jun Zhu. Cluster alignment with a teacher for unsupervised domain adaptation. In *Proceedings of the IEEE/CVF international conference on computer vision*, pages 9944–9953, 2019. 2
- [13] Ning Ding, Yixing Xu, Yehui Tang, Chao Xu, Yunhe Wang, and Dacheng Tao. Source-free domain adaptation via distribution estimation. In *Proceedings of the IEEE/CVF Conference on Computer Vision and Pattern Recognition*, pages 7212–7222, 2022. 6
- [14] Geoffrey French, Michal Mackiewicz, and Mark Fisher. Self-ensembling for visual domain adaptation. *arXiv preprint arXiv:1706.05208*, 2017. 6
- [15] Yaroslav Ganin and Victor Lempitsky. Unsupervised domain adaptation by backpropagation. In *International conference on machine learning*, pages 1180–1189. PMLR, 2015. 1, 2
- [16] Chuan Guo, Geoff Pleiss, Yu Sun, and Kilian Q Weinberger. On calibration of modern neural networks. In *International conference on machine learning*, pages 1321–1330. PMLR, 2017. 7
- [17] Kaiming He, Xiangyu Zhang, Shaoqing Ren, and Jian Sun. Identity mappings in deep residual networks. In *Computer Vision—ECCV 2016: 14th European Conference, Amsterdam, The Netherlands, October 11–14, 2016, Proceedings, Part IV 14*, pages 630–645. Springer, 2016. 5
- [18] Kaiming He, Haoqi Fan, Yuxin Wu, Saining Xie, and Ross Girshick. Momentum contrast for unsupervised visual representation learning. In *Proceedings of the IEEE/CVF conference on computer vision and pattern recognition*, pages 9729–9738, 2020. 2, 5
- [19] Tao He, Leqi Shen, Yuchen Guo, Guiguang Ding, and Zhenhua Guo. Secret: Self-consistent pseudo label refinement for unsupervised domain adaptive person re-identification. In *Proceedings of the AAAI conference on artificial intelligence*, pages 879–887, 2022. 2
- [20] Shell Xu Hu, Pablo G Moreno, Yang Xiao, Xi Shen, Guillaume Obozinski, Neil D Lawrence, and Andreas Damianou. Empirical bayes transductive meta-learning with synthetic gradients. *arXiv preprint arXiv:2004.12696*, 2020. 6
- [21] Zeyi Huang, Haohan Wang, Eric P Xing, and Dong Huang. Self-challenging improves cross-domain generalization. In *Computer Vision—ECCV 2020: 16th European Conference, Glasgow, UK, August 23–28, 2020, Proceedings, Part II 16*, pages 124–140. Springer, 2020. 8

- [22] Tri Huynh, Simon Kornblith, Matthew R Walter, Michael Maire, and Maryam Khademi. Boosting contrastive self-supervised learning with false negative cancellation. In *Proceedings of the IEEE/CVF winter conference on applications of computer vision*, pages 2785–2795, 2022. 5
- [23] Sergey Ioffe and Christian Szegedy. Batch normalization: Accelerating deep network training by reducing internal covariate shift. In *International conference on machine learning*, pages 448–456. pmlr, 2015. 5
- [24] Yusuke Iwasawa and Yutaka Matsuo. Test-time classifier adjustment module for model-agnostic domain generalization. *Advances in Neural Information Processing Systems*, 34:2427–2440, 2021. 6
- [25] Ying Jin, Ximei Wang, Mingsheng Long, and Jianmin Wang. Minimum class confusion for versatile domain adaptation. In *Computer Vision—ECCV 2020: 16th European Conference, Glasgow, UK, August 23–28, 2020, Proceedings, Part XXI 16*, pages 464–480. Springer, 2020. 6
- [26] Guoliang Kang, Lu Jiang, Yi Yang, and Alexander G Hauptmann. Contrastive adaptation network for unsupervised domain adaptation. In *Proceedings of the IEEE/CVF conference on computer vision and pattern recognition*, pages 4893–4902, 2019. 6
- [27] Nazmul Karim, Niluthpol Chowdhury Mithun, Abhinav Ravivanshi, Han-pang Chiu, Supun Samarasekera, and Nazanin Rahnavard. C-sfda: A curriculum learning aided self-training framework for efficient source free domain adaptation. In *Proceedings of the IEEE/CVF Conference on Computer Vision and Pattern Recognition*, pages 24120–24131, 2023. 1, 2, 6, 7
- [28] Sungnyun Kim, Gihun Lee, Sangmin Bae, and Se-Young Yun. Mixco: Mix-up contrastive learning for visual representation. *arXiv preprint arXiv:2010.06300*, 2020. 5
- [29] Lingjing Kong, Shaoan Xie, Weiran Yao, Yujia Zheng, Guangyi Chen, Petar Stojanov, Victor Akinwande, and Kun Zhang. Partial disentanglement for domain adaptation. In *International Conference on Machine Learning*, pages 11455–11472. PMLR, 2022. 6
- [30] Chen-Yu Lee, Tanmay Batra, Mohammad Haris Baig, and Daniel Ulbricht. Sliced wasserstein discrepancy for unsupervised domain adaptation. In *Proceedings of the IEEE/CVF conference on computer vision and pattern recognition*, pages 10285–10295, 2019. 2
- [31] Jonghyun Lee, Dahyun Jung, Junho Yim, and Sungroh Yoon. Confidence score for source-free unsupervised domain adaptation. In *International Conference on Machine Learning*, pages 12365–12377. PMLR, 2022. 2, 6
- [32] Da Li, Yongxin Yang, Yi-Zhe Song, and Timothy M Hospedales. Deeper, broader and artier domain generalization. In *Proceedings of the IEEE international conference on computer vision*, pages 5542–5550, 2017. 5
- [33] Ruihuang Li, Xu Jia, Jianzhong He, Shuaijun Chen, and Qinghua Hu. T-svdnet: Exploring high-order prototypical correlations for multi-source domain adaptation. In *Proceedings of the IEEE/CVF International Conference on Computer Vision*, pages 9991–10000, 2021. 6
- [34] Jian Liang, Dapeng Hu, and Jiashi Feng. Do we really need to access the source data? source hypothesis transfer for unsupervised domain adaptation. In *International conference on machine learning*, pages 6028–6039. PMLR, 2020. 1, 2, 5, 6
- [35] Jian Liang, Dapeng Hu, Yunbo Wang, Ran He, and Jiashi Feng. Source data-absent unsupervised domain adaptation through hypothesis transfer and labeling transfer. *IEEE Transactions on Pattern Analysis and Machine Intelligence*, 44(11): 8602–8617, 2021. 6
- [36] Mattia Litrico, Alessio Del Bue, and Pietro Morerio. Guiding pseudo-labels with uncertainty estimation for source-free unsupervised domain adaptation. In *Proceedings of the IEEE/CVF Conference on Computer Vision and Pattern Recognition*, pages 7640–7650, 2023. 1, 2, 5, 6
- [37] Mingsheng Long, Han Zhu, Jianmin Wang, and Michael I Jordan. Unsupervised domain adaptation with residual transfer networks. *Advances in neural information processing systems*, 29, 2016. 1, 2
- [38] Mingsheng Long, Zhangjie Cao, Jianmin Wang, and Michael I Jordan. Conditional adversarial domain adaptation. *Advances in neural information processing systems*, 31, 2018. 2
- [39] Divyat Mahajan, Shruti Tople, and Amit Sharma. Domain generalization using causal matching. In *International Conference on Machine Learning*, pages 7313–7324. PMLR, 2021. 8
- [40] Ke Mei, Chuang Zhu, Jiaqi Zou, and Shanghang Zhang. Instance adaptive self-training for unsupervised domain adaptation. In *Computer Vision—ECCV 2020: 16th European Conference, Glasgow, UK, August 23–28, 2020, Proceedings, Part XXVI 16*, pages 415–430. Springer, 2020. 2
- [41] Harvey B Mitchell and Paul A Schaefer. A “soft” k-nearest neighbor voting scheme. *International journal of intelligent systems*, 16(4):459–468, 2001. 3
- [42] Zak Murez, Soheil Kolouri, David Kriegman, Ravi Ramamoorthi, and Kyungnam Kim. Image to image translation for domain adaptation. In *Proceedings of the IEEE conference on computer vision and pattern recognition*, pages 4500–4509, 2018. 2
- [43] Jaemin Na, Heechul Jung, Hyung Jin Chang, and Wonjun Hwang. Fixbi: Bridging domain spaces for unsupervised domain adaptation. In *Proceedings of the IEEE/CVF conference on computer vision and pattern recognition*, pages 1094–1103, 2021. 4
- [44] Hyeonseob Nam, HyunJae Lee, Jongchan Park, Wonjun Yoon, and Donggeun Yoo. Reducing domain gap by reducing style bias. In *Proceedings of the IEEE/CVF Conference on Computer Vision and Pattern Recognition*, pages 8690–8699, 2021. 2
- [45] Alexandru Niculescu-Mizil and Rich Caruana. Predicting good probabilities with supervised learning. In *Proceedings of the 22nd international conference on Machine learning*, pages 625–632, 2005. 7, 8
- [46] Aaron van den Oord, Yazhe Li, and Oriol Vinyals. Representation learning with contrastive predictive coding. *arXiv preprint arXiv:1807.03748*, 2018. 5
- [47] Xingchao Peng, Ben Usman, Neela Kaushik, Judy Hoffman, Dequan Wang, and Kate Saenko. Visda: The visual domain adaptation challenge. *arXiv preprint arXiv:1710.06924*, 2017. 5

- [48] Xingchao Peng, Qinxun Bai, Xide Xia, Zijun Huang, Kate Saenko, and Bo Wang. Moment matching for multi-source domain adaptation. In *Proceedings of the IEEE/CVF international conference on computer vision*, pages 1406–1415, 2019. 5
- [49] Douglas A Reynolds et al. Gaussian mixture models. *Encyclopedia of biometrics*, 741(659-663), 2009. 3
- [50] Kuniaki Saito, Kohei Watanabe, Yoshitaka Ushiku, and Tatsuya Harada. Maximum classifier discrepancy for unsupervised domain adaptation. In *Proceedings of the IEEE conference on computer vision and pattern recognition*, pages 3723–3732, 2018. 1, 2
- [51] Kuniaki Saito, Donghyun Kim, Stan Sclaroff, Trevor Darrell, and Kate Saenko. Semi-supervised domain adaptation via minimax entropy. In *Proceedings of the IEEE/CVF international conference on computer vision*, pages 8050–8058, 2019. 5
- [52] Tim Salimans and Durk P Kingma. Weight normalization: A simple reparameterization to accelerate training of deep neural networks. *Advances in neural information processing systems*, 29, 2016. 5
- [53] Maohao Shen, Yuheng Bu, and Gregory W Wornell. On balancing bias and variance in unsupervised multi-source-free domain adaptation. In *International Conference on Machine Learning*, pages 30976–30991. PMLR, 2023. 1
- [54] Hui Tang, Ke Chen, and Kui Jia. Unsupervised domain adaptation via structurally regularized deep clustering. In *Proceedings of the IEEE/CVF conference on computer vision and pattern recognition*, pages 8725–8735, 2020. 2
- [55] Eric Tzeng, Judy Hoffman, Kate Saenko, and Trevor Darrell. Adversarial discriminative domain adaptation. In *Proceedings of the IEEE conference on computer vision and pattern recognition*, pages 7167–7176, 2017. 2
- [56] Laurens Van der Maaten and Geoffrey Hinton. Visualizing data using t-sne. *Journal of machine learning research*, 9(11), 2008. 7, 8
- [57] Vladimir N. Vapnik. *Statistical Learning Theory*. Wiley-Interscience, 1998. 8
- [58] Dequan Wang, Evan Shelhamer, Shaoteng Liu, Bruno Olshausen, and Trevor Darrell. Tent: Fully test-time adaptation by entropy minimization. *arXiv preprint arXiv:2006.10726*, 2020. 1, 2, 6
- [59] Qian Wang and Toby Breckon. Unsupervised domain adaptation via structured prediction based selective pseudo-labeling. In *Proceedings of the AAAI conference on artificial intelligence*, pages 6243–6250, 2020. 2
- [60] Shuai Wang, Daoan Zhang, Zipei Yan, Jianguo Zhang, and Rui Li. Feature alignment and uniformity for test time adaptation. In *Proceedings of the IEEE/CVF Conference on Computer Vision and Pattern Recognition*, pages 20050–20060, 2023. 6, 8
- [61] Garrett Wilson and Diane J Cook. A survey of unsupervised deep domain adaptation. *ACM Transactions on Intelligent Systems and Technology (TIST)*, 11(5):1–46, 2020. 1
- [62] Qinwei Xu, Ruipeng Zhang, Ya Zhang, Yanfeng Wang, and Qi Tian. A fourier-based framework for domain generalization. In *Proceedings of the IEEE/CVF Conference on Computer Vision and Pattern Recognition*, pages 14383–14392, 2021. 8
- [63] Renjun Xu, Pelen Liu, Liyan Wang, Chao Chen, and Jindong Wang. Reliable weighted optimal transport for unsupervised domain adaptation. In *Proceedings of the IEEE/CVF conference on computer vision and pattern recognition*, pages 4394–4403, 2020. 6
- [64] Shiqi Yang, Joost van de Weijer, Luis Herranz, Shangling Jui, et al. Exploiting the intrinsic neighborhood structure for source-free domain adaptation. *Advances in neural information processing systems*, 34:29393–29405, 2021. 1, 6
- [65] Shiqi Yang, Yaxing Wang, Joost Van De Weijer, Luis Herranz, and Shangling Jui. Generalized source-free domain adaptation. In *Proceedings of the IEEE/CVF International Conference on Computer Vision*, pages 8978–8987, 2021. 6
- [66] Shiqi Yang, Shangling Jui, Joost van de Weijer, et al. Attracting and dispersing: A simple approach for source-free domain adaptation. *Advances in Neural Information Processing Systems*, 35:5802–5815, 2022. 2, 6
- [67] Xufeng Yao, Yang Bai, Xinyun Zhang, Yuechen Zhang, Qi Sun, Ran Chen, Ruiyu Li, and Bei Yu. Pcl: Proxy-based contrastive learning for domain generalization. In *Proceedings of the IEEE/CVF Conference on Computer Vision and Pattern Recognition*, pages 7097–7107, 2022. 8
- [68] Yu-Chu Yu and Hsuan-Tien Lin. Semi-supervised domain adaptation with source label adaptation. In *Proceedings of the IEEE/CVF Conference on Computer Vision and Pattern Recognition*, pages 24100–24109, 2023. 2
- [69] Hongyi Zhang, Moustapha Cisse, Yann N Dauphin, and David Lopez-Paz. mixup: Beyond empirical risk minimization. *arXiv preprint arXiv:1710.09412*, 2017. 3
- [70] Pan Zhang, Bo Zhang, Ting Zhang, Dong Chen, Yong Wang, and Fang Wen. Prototypical pseudo label denoising and target structure learning for domain adaptive semantic segmentation. In *Proceedings of the IEEE/CVF conference on computer vision and pattern recognition*, pages 12414–12424, 2021. 1
- [71] Weichen Zhang, Wanli Ouyang, Wen Li, and Dong Xu. Collaborative and adversarial network for unsupervised domain adaptation. In *Proceedings of the IEEE conference on computer vision and pattern recognition*, pages 3801–3809, 2018. 2
- [72] Wenqiao Zhang, Lei Zhu, James Hallinan, Shengyu Zhang, Andrew Makmur, Qingpeng Cai, and Beng Chin Ooi. Boostmis: Boosting medical image semi-supervised learning with adaptive pseudo labeling and informative active annotation. In *Proceedings of the IEEE/CVF Conference on Computer Vision and Pattern Recognition*, pages 20666–20676, 2022. 1
- [73] Yixin Zhang, Zilei Wang, and Weinan He. Class relationship embedded learning for source-free unsupervised domain adaptation. In *Proceedings of the IEEE/CVF Conference on Computer Vision and Pattern Recognition*, pages 7619–7629, 2023. 1, 2
- [74] Ziyi Zhang, Weikai Chen, Hui Cheng, Zhen Li, Siyuan Li, Liang Lin, and Guanbin Li. Divide and contrast: Source-free domain adaptation via adaptive contrastive learning. *Advances in Neural Information Processing Systems*, 35:5137–5149, 2022. 5
- [75] Yang Zou, Zhiding Yu, BVK Kumar, and Jinsong Wang. Unsupervised domain adaptation for semantic segmentation via

class-balanced self-training. In *Proceedings of the European conference on computer vision (ECCV)*, pages 289–305, 2018.

2